pubs.acs.org/acschemicalbiology

Articles

Shaping Neonatal Immunization by Tuning the Delivery of Synergistic Adjuvants via Nanocarriers

Soumik Barman, Francesco Borriello,[⋈] Byron Brook,[⋈] Carlo Pietrasanta,[⋈] Maria De Leon, Cali Sweitzer, Manisha Menon, Simon D. van Haren, Dheeraj Soni, Yoshine Saito, Etsuro Nanishi, Sijia Yi, Sharan Bobbala, Ofer Levy, Evan A. Scott,* and David J. Dowling*

Cite This: *ACS Chem. Biol.* 2022, 17, 2559–2571

Read Online

ACCESS | Metrics & More | Article Recommendations | Supporting Information

ABSTRACT: Adjuvanted nanocarrier-based vaccines hold substantial potential for applications in novel early-life immunization strategies. Here, via mouse and human age-specific in vitro modeling, we identified the combination of a small-molecule STING agonist (2′3′-cyclic GMP-AMP, cGAMP) and a TLR7/8 agonist (CL075) to drive the synergistic activation of neonatal dendritic cells and precision CD4 T-helper (Th) cell expansion via the IL-12/IFNγ axis. We further demonstrate that the vaccination of neonatal mice with quadrivalent influenza recombinant hemagglutinin (rHA) and an admixture of two polymersome (PS) nanocarriers separately encapsulating cGAMP (cGAMP-PS) and CL075 (CL075-PS) drove robust Th1 bias, high frequency of T follicular helper (T_{FH}) cells, and germinal center (GC) B cells along with the IgG2c-skewed humoral response in vivo. Dual-loaded cGAMP/CL075-PSs did not outperform admixed cGAMP-PS and CL075-PS in vivo. These data validate an optimally designed adjuvantation system via age-selected small-molecule synergy and a multicomponent nanocarrier formulation as an effective approach to induce type 1 immune responses in early life.

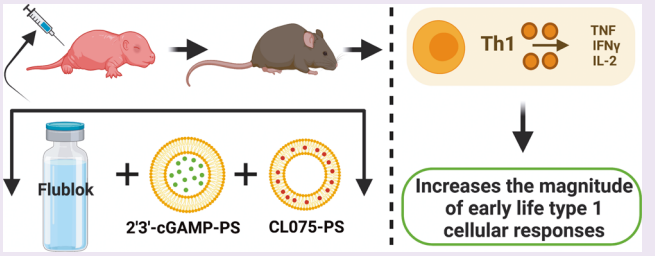

INTRODUCTION

New vaccine strategies and formulations are needed to provide improved protection for vulnerable populations, such as infants and older adults (i.e., elderly).[1] Adjuvants are critical components of vaccine formulations that can significantly increase immunization efficacy, primarily by functioning as agonists of pattern-recognition receptors (PRRs) to stimulate innate immune cells. However, most adjuvanted vaccine formulations are not rationally selected or tailored to account for age-associated differences in innate immune responses, often resulting in suboptimal hyporesponsiveness and/or immunosenescent differences in translational vaccine outcomes.[2,3] Strategies under consideration to address these distinct responses include (a) combining two or more PRR agonists into a single vaccine[4] and (b) optimization of immune-engineering strategy and delivery system design in an age-specific manner.[5,6] Immunomodulation and intracellular delivery of antigen/adjuvant by nanocarriers comprised of poly(ethylene glycol)-*b*-poly(propylene sulfide) (PEG-*b*-PPS) block copolymers have been well characterized.[7−11] PEG-*b*-PPS nanocarrier platforms permit the efficient loading of not only both hydrophobic and hydrophilic adjuvants[7−11] but also prime T cells by enhancing their uptake and presentation by antigen presenting cells (APCs).[7−11]

Our group has previously employed adjuvant-loaded PEG-*b*-PPS polymersome (PS) nanocarriers[12] to enable delivery to specific subsets of leukocytes (i.e., directly to APCs) and even specific subcellular compartments (i.e., endosomes). This strategy is highly advantageous for the selective targeting of endosomal receptors, such as Toll-like receptor (TLR)7 and TLR8, and cytosolic receptors like stimulator of interferon genes (STING).[13] We demonstrated that TLR7/8 agonist PS formulations mimic the immunomodulating effects of the live attenuated vaccine Bacille Calmette-Guérin (BCG), which is commonly given to newborns in tuberculosis-endemic countries, by enhancing both innate and adaptive immune responses.[12] Notably, when coloaded with the *Mycobacterium tuberculosis* antigen 85B peptide 25, the TLR8 agonist-loaded PSs were comparable to BCG in inducing antigen-specific immune responses in hTLR8-expressing humanized neonatal mice in vivo.[12] Furthermore, we discovered that cGAMP is a potent activator of newborn dendritic cells (DCs).[13] As compared to alum or cGAMP alone, immunization with cGAMP adsorbed onto alum via inherent phosphonate groups, enhanced murine newborn rHA-specific IgG2a/c titers, an

Received: June 10, 2022
Accepted: August 15, 2022
Published: August 26, 2022

https://doi.org/10.1021/acschembio.2c00497
ACS Chem. Biol. 2022, 17, 2559−2571

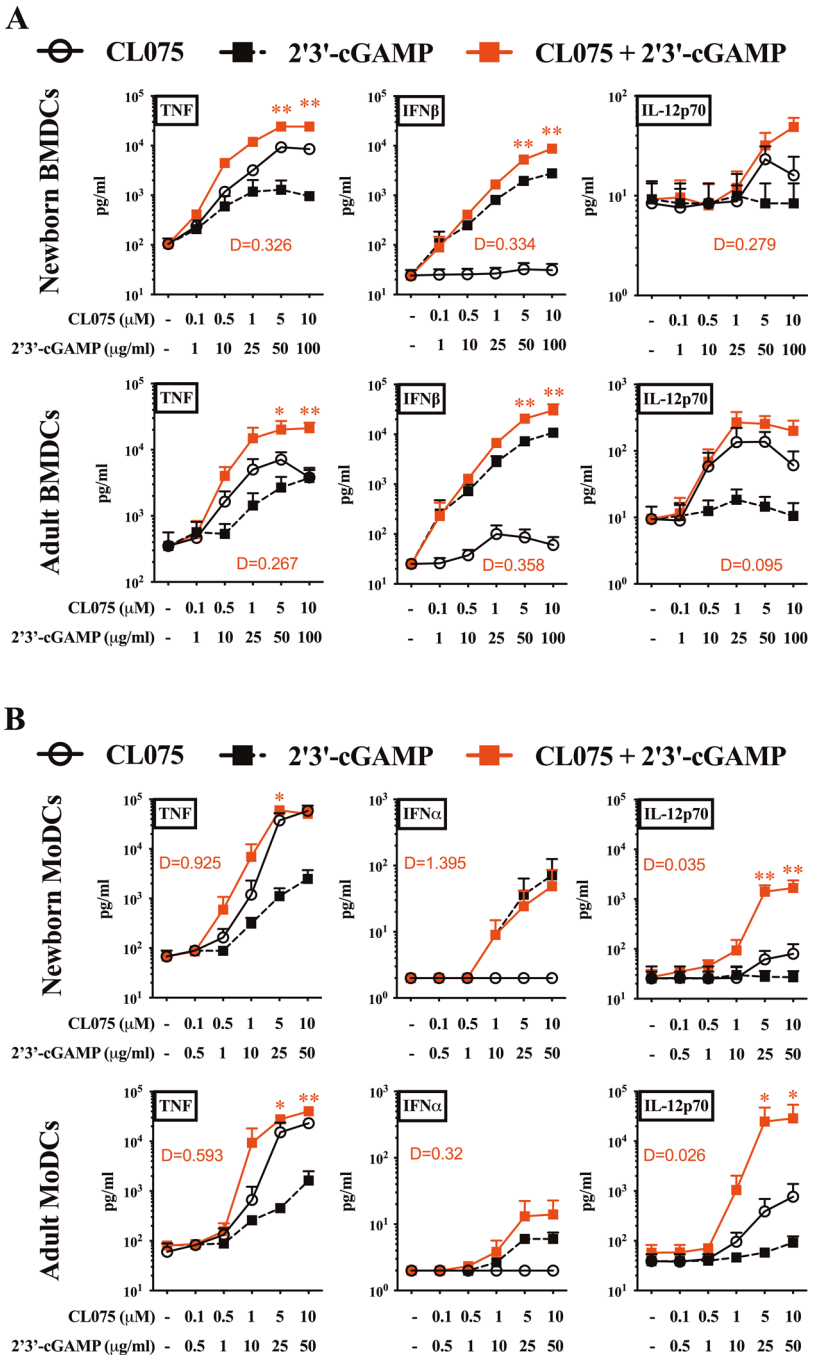

Figure 1. cGAMP and CL075 synergistically induced Th1-related cytokines in murine and human dendritic cells. (A) BMDCs from newborn (7 days of life) and adult (~8 weeks old) mice and (B) MoDCs from human neonatal CBMC and adult PBMC were stimulated with the indicated concentration of 2′3′-cGAMP and CL075. Degree of synergy (D) was compared between groups using an adapted Loewe definition of additivity ($D < 1$, synergy; $D = 1$, additivity; $D > 1$, antagonism). Data were representative of three independent experiments. Statistical comparison was performed using two-way ANOVA corrected for multiple comparisons; $*p < 0.033$, $**p < 0.002$ ($n = 7$ per group).

antibody (Ab) subclass associated with the development of interferon (IFN)γ-driven type 1 immunity in vivo, and endowed with higher effector functions.[13] Hence, we hypothesized that targeting both STING and TLR7/8 pathways in early-life innate immune cells could be a promising precision vaccinology strategy.

In the present study, we identify that a combination of small molecules cGAMP and CL075 drive synergistic and robust activation of neonatal dendritic cells and precision of CD4 Th cell expansion via the IL-12/IFNγ axis in vitro. Then, we took advantage of the standardized PS platform to formulate separate cGAMP- and CL075-loaded PSs (cGAMP-PS and CL075-PS) and studied tunable aspects of immunomodulation in early-life immunization with the help of the quadrivalent influenza subunit vaccine, Flublok in vivo. We also coencapsulated CL075 and cGAMP inside PSs and assessed the differences in the resulting kinetics and immunostimulatory effects. Admixture of CL075-PS and cGAMP-PS primed rHA-specific T_{FH} and GC B cell responses and induced robust humoral and rHA-specific Th1 and $CD8^+$ T cell responses.

https://doi.org/10.1021/acschembio.2c00497
ACS Chem. Biol. 2022, 17, 2559−2571

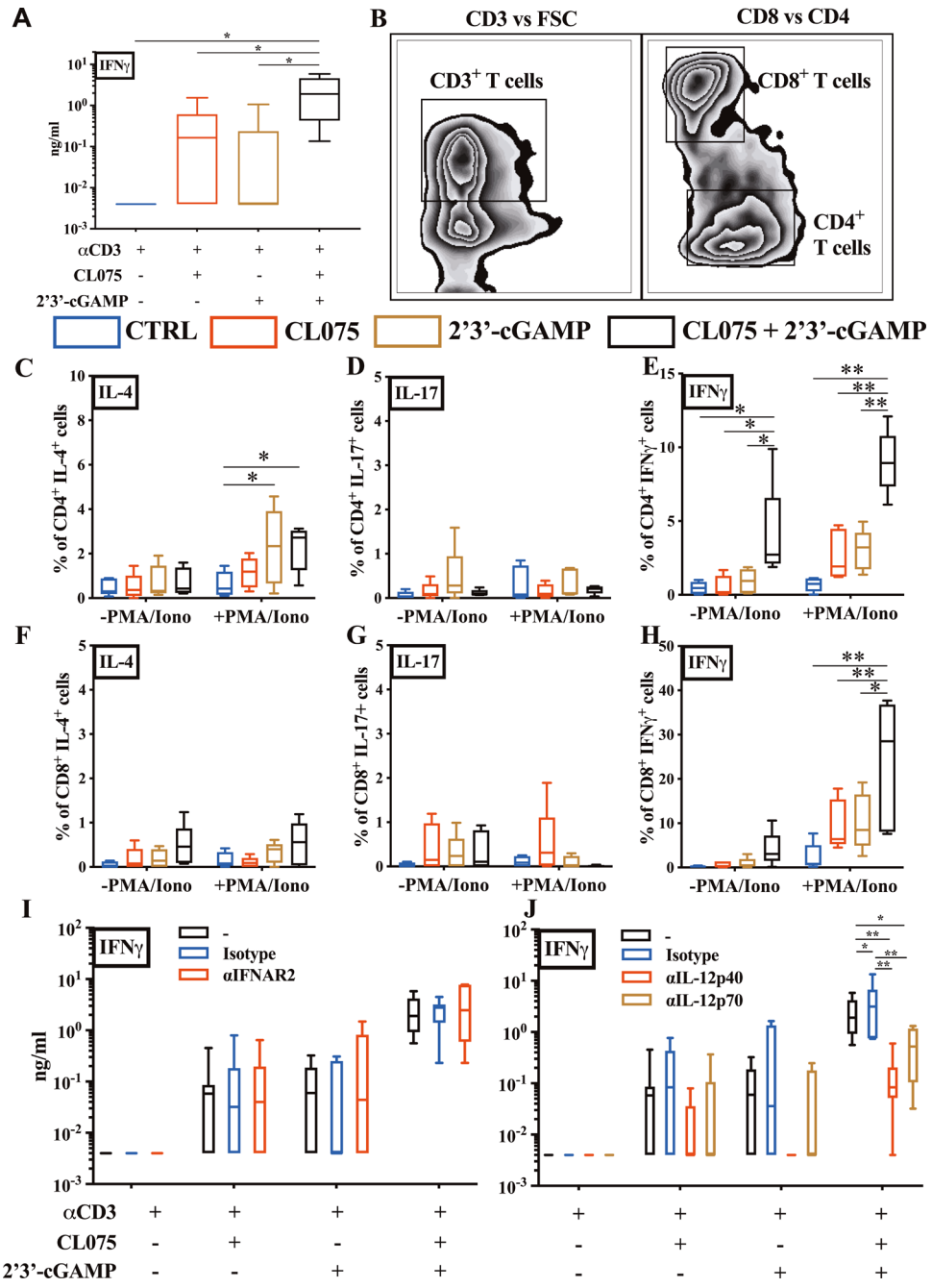

Figure 2. Combination of cGAMP and CL075 drove IL-12-dependent Th1 polarization in human neonatal T cells. (A) Neonatal CBMCs were cultured in vitro for 96 h in the presence of polyclonal T cell activator α-CD3 (1 μg/mL) with or without CL075 (5 μM), cGAMP (25 μg/mL), or cGAMP + CL075, followed by IFNγ production evaluation by ELISA. (B) Example gating strategy for the quantification of $CD4^+$ and $CD8^+$ T cells. (C−H) CBMCs were cultured in vitro as in panel (A) but with the addition of a mitogen and cytokine blocker for the last 6 h. After stimulation, cells were harvested, stained (intracellular cytokine staining), and analyzed by flow cytometry to quantify the percentage of T cells producing IL-4, IL-17, and IFNγ. (I) CBMCs were cultured in vitro as in panel (A) but with the addition of human blocking Abs, αIFNAR2, or (J) αIL-12p40/70. After stimulation, the collected supernatant was evaluated via ELISA for IFNγ. Data were representative of two independent experiments. Statistical comparison employed test one or two-way ANOVA corrected for multiple comparisons; $*p < 0.033$, $**p < 0.002$ ($n = 7$ per group).

Using the PS platform and the combination of STING and TLR7/8 agonists, we successfully enhanced rHA-specific type 1 immunity in infant mice. Within a framework of precision vaccinology, the formulation of such precision adjuvant delivery systems to fine-tune vaccine immunogenicity may inform the development of next-generation rationally designed vaccines for vulnerable pediatric and elder human populations.

RESULTS AND DISCUSSION

Dual STING and TLR7/8 Stimulation Drive IL-12-Dependent Th1 Polarization in Early Life. STING[13−15] and TLR7/8[12,16,17] agonists induce overlapping but distinct innate immunological profiles,[18] with both upstream activation pathways leading to the secretion of innate type 1 interferon and proinflammatory cytokine production. These cytokines are

https://doi.org/10.1021/acschembio.2c00497
ACS Chem. Biol. 2022, 17, 2559−2571

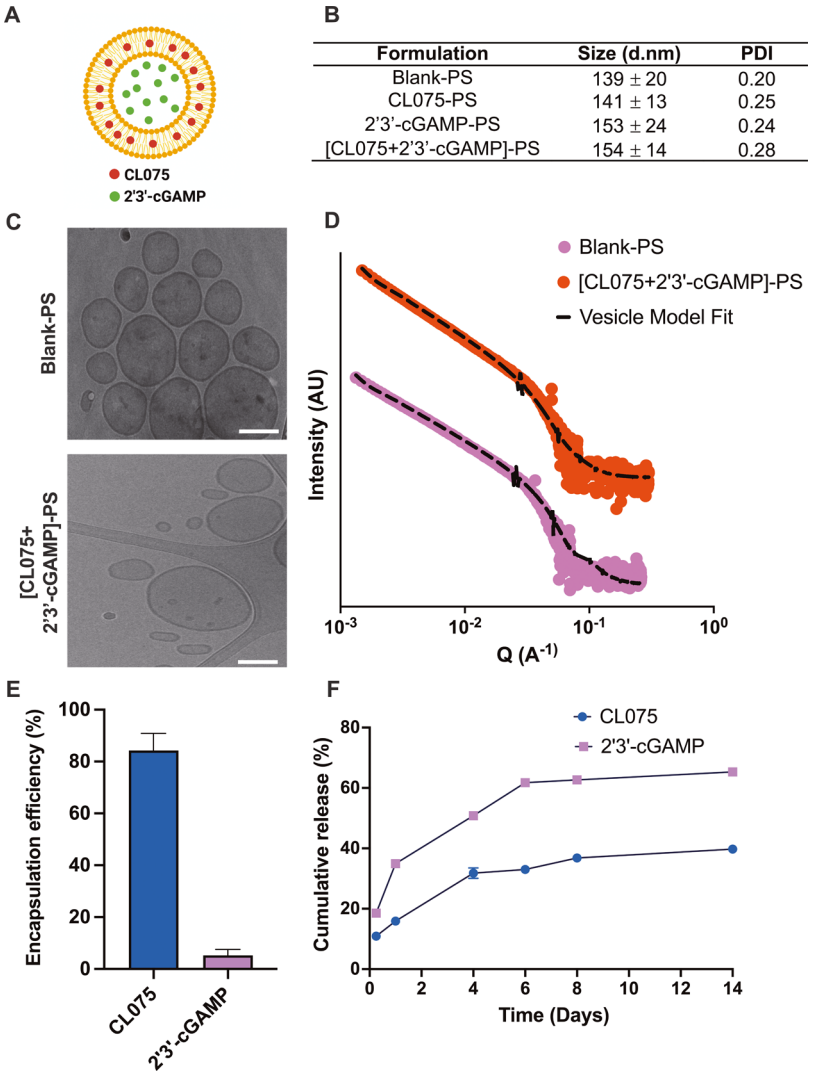

Figure 3. cGAMP and CL075 encapsulation and characterization of adjuvant-loaded PEG-*b*-PPS polymersomes. (A) Schematic showing adjuvant-loaded-PEG-*b*-PPS PSs, with hydrophobic CL075 in the PS bilayer membrane and hydrophilic cGAMP in the aqueous core. (B) Dynamic light scattering analysis of blank and adjuvant-loaded PS formulations. Size (d nm) and polydispersity index (PDI) were reported as mean ± SD (n = 3). (C) Representative cryo-TEM images of blank-PS and dual adjuvant-loaded PS ((CL075 + cGAMP)-PS). TEM images were acquired at ×10 000 magnification (scale = 100 nm). (D) Small-angle X-ray scattering (SAXS) profile and model fits for blank-PS and dual adjuvant-loaded PS ((CL075 + cGAMP)-PS). The scattering profile and vesicle model fit are represented as solid dots and dotted lines, respectively. (E) Encapsulation of CL075 and cGAMP in PS. The encapsulation of adjuvants was measured after purifying PS with size exclusion chromatography. Encapsulation efficiency (%) was reported as mean ± SD (n = 3). (F) In vitro release of CL075 and 2′3′-cGAMP from PS over 2 weeks (14 days). Release studies were performed in phosphate-buffered saline (pH 7.4) at 37 °C. Cumulative release (%) was reported as mean ± SD (n = 3).

critical to APC priming of T cells and the initiation of adaptive immune responses. To assess the immunostimulatory profiles and synergistic effects of cGAMP and CL075 on primary dendritic cells (DCs) from murine and human origins, we stimulated adult and neonatal bone marrow-derived dendritic cells (BMDCs) from mice (Figure 1A) and human monocyte-derived dendritic cells (MoDCs) (Figure 1B) with increasing concentrations of each small-molecule agonist for 24 h. The concentrations used for cGAMP and CL075 were determined based on prior dose-titration experiments,[13,19,20] which were focused on maximal cytokine/interferon induction and DC maturation,[13] along with initial limitations in adjuvant encapsulation into PS (unpublished observations). Next, we focused on TNF, IFNβ, and IL-12p70 as surrogates for the capacity to induce a Th1-promoting innate response. CL075 and cGAMP synergistically induced the concentration-dependent TNF and IFNβ productions in neonatal and adult BMDCs (Figure 1A). A similar pattern was observed for the production of TNF and IL-12p70 by neonatal and adult human MoDCs (Figure 1B). Overall, the highest degree of synergy was noted for IL-12p70. Specifically, the combined treatment with cGAMP and CL075 overcame neonatal DC hyporesponsiveness for IL-12p70 production, of which neonatal DCs are known to have a limited production ability in response to most PRR agonists.[21−23] This hyporesponsiveness, combined with a baseline Th2-polarized response,[24−26] contributes to the distinctness of neonatal DCs.

To evaluate the synergy between two biological agents, researchers have advocated for the use of an "interaction barometer", comparing different drug combinations for the degree of interaction between individual components alone and their combined responses.[27] Any synergy model should be

https://doi.org/10.1021/acschembio.2c00497
ACS Chem. Biol. 2022, 17, 2559−2571

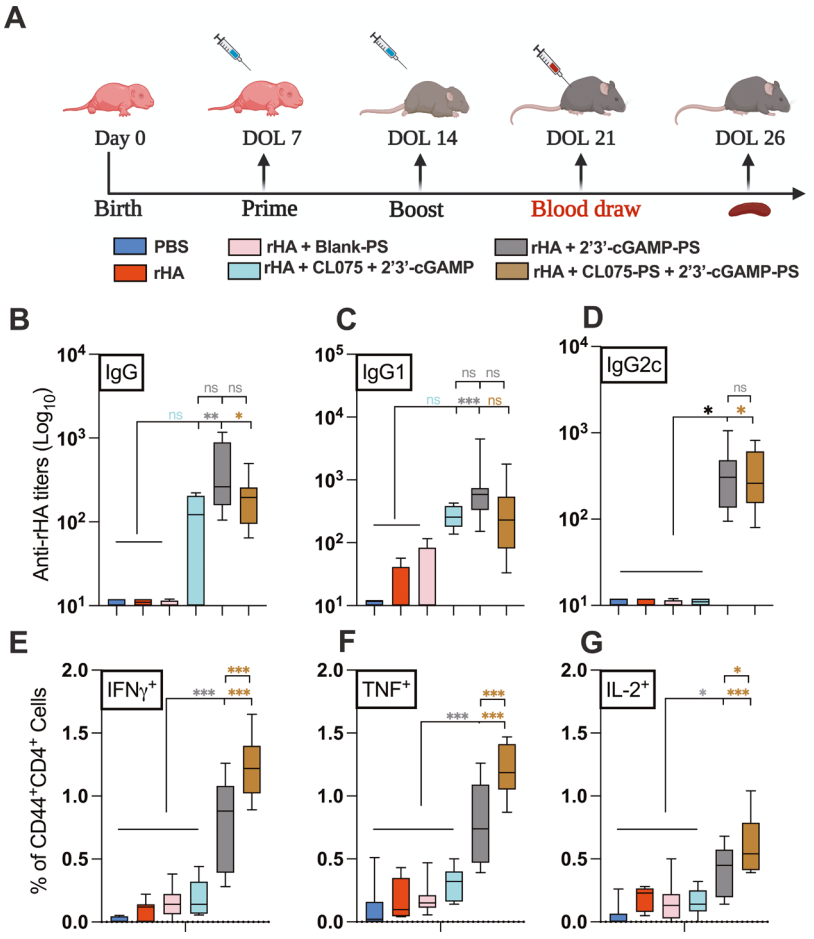

Figure 4. Individually encapsulated cGAMP and admixed cGAMP and CL075-PSs enhanced rHA-specific neonatal humoral and cell-mediated immune responses. (A) Infant C57BL/6 mice were immunized i.m. on DOL (day of life) 7 and 14. All groups received 1 μg of each of the Flublok quadrivalent antigens (rHA), except the PBS group. rHA was given alone or in combination with cGAMP (1 μg) and CL075 (164 μM) delivered in admixture or single-loaded or dual-loaded PEG-*b*-PPS nanocarriers. (B) Antibody titers for rHA-specific IgG (B), IgG1(C), and IgG2c (D) were determined by ELISA in serum samples collected at DOL 21. (E−G) Murine $CD4^+$ T cell responses after rHA stimulation. Splenocytes from rHA and adjuvanted vaccinates were isolated, stimulated with 10 μg/mL of Flublok along with CD28 (1 μg/mL) and CD49d (1 μg/mL) for 12 h followed by 6 h of BFA stimulation to block the extracellular cytokine secretion. After stimulation, cells were harvested, stained (intracellular cytokine staining), and analyzed by flow cytometry. Plots were gated on $CD44^+$ $CD4^+$ lymphocytes and analyzed for all combinations of simultaneous IFNγ, TNF, and IL-2 productivity. Statistical comparison was performed either using one-way ANOVA or nonparametric Kruskal-Wallis test corrected for multiple comparisons; ns denoted non-significant, $^*p < 0.033$, $^{**}p < 0.002$, $^{***}p < 0.001$ ($n = 5-12$ per group). The study was inclusive of two independent repeats.

treated as an exploratory ranking statistic, as opposed to a probability or effect statistic, for prioritization of the most potent combinations for further evaluation, rather than a "true model" for explaining synergy or antagonism mechanisms. One such adaptation, used here, is the Loewe method of additivity[28−30] to assess whether cytokine/interferon production after stimulation with agonist combinations was synergistic, additive, or antagonistic. As such, while other models may give a slightly divergent ranking, the actionability of this approach favors its use in the discovery phase.

Next, we employed a 96 h human newborn T-helper polarization assay, which leverages the intrinsic characteristics of the newborn T cell compartment (composed mainly of naïve T cells) to iteratively characterize how adjuvant and nanocarrier formulation modulate T cell polarization in mixed mononuclear cell culture in the presence of a TCR-mediated stimulus. Cord blood mononuclear cells (CBMCs) were stimulated with αCD3 (polyclonal T cell activator) ± CL075 (5 μM), cGAMP (25 μg/mL), or combined, and the selective contribution of different factors (e.g., type I IFNs, IL-12p70) to T cell polarization was investigated via blocking Abs. Interestingly, and in line with DC data, we observed a restored Th1 predominance in neonatal leukocytes via the combination of CL075 and cGAMP (Figure 2A). To investigate further, we confirmed the accumulation of IFNγ^+ $CD4^+$ (Th1-polarized) neonatal T cells, minimal IL-4^+ but not IL-17^+, in the presence of both CL075 and cGAMP by flow cytometry (Figure 2B−E). The IFNγ response was significant both without or with TCR stimulation. IFNγ^+ $CD8^+$ neonatal T cells were detected upon the combined stimulation of TLR7/8 and STING agonists (Figure 2B,F−H), with significant changes observed only in the presence of TCR stimulation. Importantly, using neutralizing Abs (nAbs) against type I IFN signaling (αIFNAR2) and combined nAbs against IL-12p40/70 (αIL-12p40/70), we demonstrated that the secretion of IFNγ^+ by CBMCs over 96 h is reliant on innate IL-12 signaling (Figure 2I−J).

https://doi.org/10.1021/acschembio.2c00497
ACS Chem. Biol. 2022, 17, 2559−2571

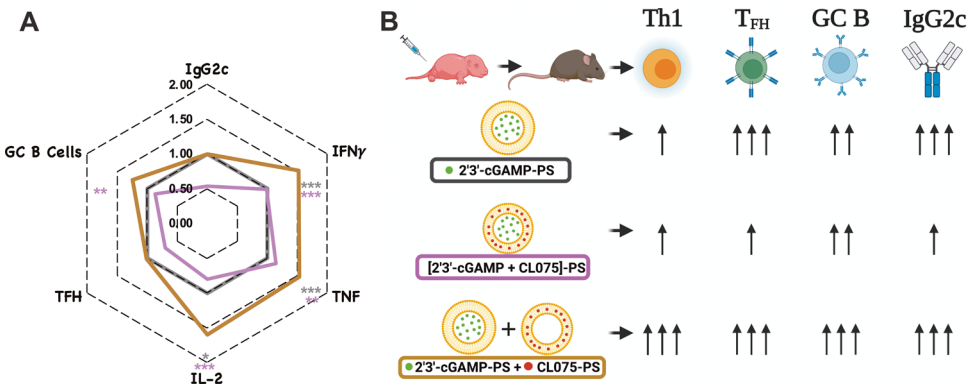

Figure 5. Adjuvanted nanocarrier formulation skews neonatal immunity toward a type 1 response. Together, cGAMP and CL075 encapsulating PSs alter rHA-specific Th1 polarization and overcome the inability of the infant immune system to mount a type 1 immunity and tune the degree of immune response enhancement. (A) The magnitude of rHA-specific IgG2c titers (at DOL 21), Th1 polarization, T_{FH}, and GC B cell responses (DOL 26) is shown in a radar plot as a fold-change over cGAMP-PS-immunized group (black line). Statistical comparison was performed either using one-way ANOVA or nonparametric Kruskal-Wallis test corrected for multiple comparisons; $*p < 0.033$, $**p < 0.002$, $***p < 0.001$ ($n = 5-12$ per group). The study was inclusive of two independent repeats. (B) Tunable aspects of different formulations when small-molecule agonists are encapsulated in PEG-*b*-PPS nanocarriers.

Synthesis and Characterization of Adjuvant-Loaded PS Nanocarriers. PEG-*b*-PPS copolymers with hydrophilic block weight fractions of 0.38 were self-assembled into PS, as previously described.[31,32] PSs were formed and loaded using the flash nanoprecipitation technique,[7,31] with the hydrophobic CL075 loaded within the PS bilayer membrane and hydrophilic cGAMP encapsulated within the aqueous core (Figure 3A). Each batch of PSs was well characterized, including the quantification of loaded adjuvant, average particle size, polydispersity, and morphology (Figure 3B). Blank and adjuvant-loaded PSs demonstrated sizes between 140 and 155 nm with a polydispersity index (PDI) of less than 0.3. Cryogenic transmission electron microscopy (Cryo-TEM) images confirmed the vesicular morphology of self-assembled PSs (Figure 3C). Small-angle X-ray scattering (SAXS) profiles of blank-PS and dual adjuvant-loaded PSs ((CL075 + cGAMP)-PS) optimally fit a vesicle model, which further verifies the vesicle morphology of nanocarrier formulations (Figure 3D). The loading of agonists into PSs was generally observed with encapsulation efficiencies of >80% for CL075 or ∼6% for cGAMP (Figure 3E). In vitro release of CL075 and cGAMP from PSs was performed over 2 weeks (14 days) in phosphate-buffered saline (pH 7.4) at 37 °C, with the cumulative release ranging from 20 to 60% (Figure 3F). The highly hydrophilic nature of cGAMP might have contributed to its lower encapsulation efficiency and greater diffusion from PS as compared to the hydrophobic CL075 that is trapped inside the PS bilayer membrane.

Admixture of cGAMP-PS and CL075-PS Enhances Th1-Polarized Ag-Specific Adaptive Responses in Young Mice. Previously, we have demonstrated that cGAMP is a promising adjuvant candidate for early-life immunization.[13] We have also demonstrated that the optimization of vaccine formulation and delivery route can enhance the adjuvanticity potential of TLR7/8 agonists (e.g., CL075),[1,3] specifically by encapsulation within PEG-*b*-PPS nanocarriers.[12] Our team has validated PEG-*b*-PPS PSs for nontoxic adjuvant delivery to mice with enhanced targeted uptake by DCs and monocytes.[10−12] To assess whether the synergy observed for the combination of cGAMP and CL075 in vitro was also evident in vivo, we next evaluated adjuvant/s-loaded PS nanocarriers in an infant mouse vaccination model. Infant mice were immunized intramuscularly (i.m.) by cGAMP (1 μg) and/or CL075 (164 μM) either alone or in an encapsulated or coencapsulated formulation (Table S1). rHA (Flublok) was used as a model antigen to assess the adaptive immune response. On day of life (DOL) 21, which was 7 days after the boost, serum was collected and analyzed for an rHA-specific humoral response (Figure 4A). Compared to the control groups (PBS, rHA, or rHA + Blank-PS), both cGAMP-PS and the PS admixture (cGAMP-PS + CL075-PS)-immunized groups showed significant induction of rHA-specific total IgG (Figure 4B), IgG1 (Figure 4C), and IgG2c (Figure 4D). The coencapsulated (cGAMP + CL075)-PS formulation did not demonstrate any superior humoral effect with rHA (Figure S1A−C). Next, we focused on the adaptive compartment of vaccine-induced immunity by harvesting splenocytes on DOL 26 (12 days after boost) and restimulated the cell suspension with vaccinal antigen (Flublok) for 18 h. The importance of Flublok-specific $CD4^+$ T cells, especially the Th1 subset, and $CD8^+$ T cells for the development of a proper anti-influenza immunity is now well established.[33,34] Of note, the admixture (cGAMP-PS + CL075-PS) formulation induced a more robust Th1 polarization upon memory recall in the infant setting (Figure 4E−G), characterized by the significant release of IFNγ (Figure 4E), TNF (Figure 4F), and IL-2 (Figure 4G) compared to control groups as well as cGAMP-PS-immunized groups. Coencapsulated formulation (cGAMP + CL075)-PS demonstrated inferior Th1 polarization upon vaccination (Figures 5 and S1D−F). A similar trend was observed in the rHA-specific $CD8^+$ T cell compartment, where admixture (cGAMP-PS + CL075-PS) triggered $IFN\gamma^+$ release (Figure S2), which has already been proven important in viral clearance upon influenza infection.[35−38] Furthermore, Flublok stimulation facilitated the triggering of a population of monofunctional $IFN\gamma^+$ $TNF^-IL\text{-}2^-$ $CD4^+$ T cells in the coencapsulated formulation-immunized group (Figure S3B).

To decipher the immunomodulatory effect of the admixture on germinal centers (GCs), we investigated the accumulation of T_{FH} cells and GC B cells, plasmablasts, and plasma cells by flow cytometry in the inguinal and popliteal draining lymph nodes (dLNs) on 12 days after the boost (Figures 5 and S4). Consistent with previous observations that TLR8 signaling evokes T_{FH} cell differentiation ex vivo[39,40] and that cGAMP

https://doi.org/10.1021/acschembio.2c00497
ACS Chem. Biol. 2022, 17, 2559−2571

with alum[13] or cGAMP-loaded virus-like particles[41] induce T_{FH} cells in dLNs of adult mice, cGAMP-PS induced $CD4^+$ T_{FH} responses, as reflected by an increase in $CD3^+CD4^+PD\text{-}1^+CXCR5^+$ T cells (Figure S4C). Despite being the inferior Th1 inducer in vivo, the coencapsulated formulation triggered similar T_{FH} responses when compared with the admixture formulation (Figure S1G). This may explain why cGAMP-PS and coencapsulated formulations act as an effective inducer of Flublok-specific humoral responses since T_{FH} differentiation has proven beneficial for inducing strong humoral immune responses.[39,40] Furthermore, the admixture (cGAMP-PS + CL075-PS) formulation triggers the frequency of GC B cells in the dLN compartment over the blank-PS control group (Figure S4D). The magnitude of rHA-specific IgG2c titers (at DOL 22), Th1 polarization, T_{FH}, and GC B cell responses (DOL 26) is depicted in a radar plot as a fold-change over the cGAMP-PS-immunized group (black line) (Figure 5A). Fascinatingly, due to lymphadenopathy (unpublished observations), cGAMP-PS-immunized group showed a remarkable accumulation of the total number of T_{FH} cells, GC B cells, plasmablasts, and plasma cells (Figure S4G–J). Together, cGAMP and CL075 encapsulating PSs alter rHA-specific Th1 polarization, overcome the inability of the infant immune system to mount a type 1 immune response, and allow tuning of the degree of immune response enhancement (Figure 5B).

CONCLUSIONS

Newborns and young infants demonstrate distinct immune ontogeny including a reduced ability to drive IFNγ-driven type 1 immunity, which, in turn, leads to a higher risk of infections with intracellular pathogens and reduced vaccine efficacy.[42,43] Although there is no comprehensive consensus on whether and how in vitro models can predict the in vivo effect of candidate adjuvants, the use of DCs has some advantages for assessing the adjuvant activity in vitro.[43−46] For example, in vitro and preclinical in vivo studies have shown that targeting endosomal and cytosolic PRRs, such as TLR7/8,[20,47−52] potently activates human newborn leukocytes and markedly enhances vaccine efficacy in neonatal nonhuman primates.[48] At the single-cell level, neonatal innate cells generally are less capable of producing multiple cytokines simultaneously, i.e., are less polyfunctional.[53] We can bypass this impairment by selecting unique PRR agonist adjuvant combinations.[20,24] As we are studying the combination of the TLR7/8 and STING agonist adjuvants, we decided to use neonatal cells and compared them directly with their adult counterparts. The advantages of such in vitro assays include cost-effectiveness and ease of sample availability. The disadvantage may be the limited ability to fully recapitulate in vivo immunological attributes.[43] In the present work, by combining an in vitro study of newborn DC activation and murine in vivo immunization model and taking advantage of a delivery system such as PEG-*b*-PPS PSs, we demonstrated the potential immunization benefit of dual STING and TLR7/8 agonist adjuvant activations in the early-life setting. Specifically, using an admixture of cGAMP-PS and CL075-PS as an adjuvantation strategy for early-life immunization, we were able to induce cardinal features of type 1 immunity: (1) IFNγ production by antigen-specific $CD4^+$ T cells and (2) relatively high titers of antigen-specific IgG2c. As IFNγ promotes isotype switching toward IgG2a/c in vivo,[54] these two effects are likely linked.

Interestingly, in our study, we did not observe any benefit from coencapsulation of cGAMP and CL075 within PS as compared with individual encapsulation and admixed agonist PSs. This may be due to the faster release kinetics of cGAMP from the encapsulated PS compared to that of CL075 due to its hydrophilic nature. Polymersomes are vesicular nanoparticles where CL075 is embedded in the hydrophobic bilayer membrane and 2′3′-cGAMP in the hydrophilic core. During polymersome endocytosis and subsequent endolysosome formation in APCs, there is an expected faster diffusion of hydrophilic 2′3′-cGAMP into the cytoplasm to activate STING as compared to hydrophobic CL075 release to activate TLR7/8 in the endosomes. As such, one possible limitation of utilizing in vitro studies with coencapsulated formulations is that it might not fully replicate the distinct controlled release kinetics, which we captured in vivo after delivering them intramuscularly. Alternatively, our admixed approach may simply generate distinct heterogeneous activated APC populations. In the case of coencapsulation, only one activated APC population would be anticipated—i.e., those receiving both cGAMP and CL075, while the admixture may generate three distinct populations: (1) APCs receiving cGAMP, (2) APCs receiving CL075, and (3) APCs receiving both cGAMP and CL075. The latter may manifest distinct immunostimulation of cGAMP and CL075.

Our study also expands upon prior materials science work,[55] where the STING agonist 3′3′-cGAMP and/or the TLR8/7 agonist R848 was encapsulated using acetylated dextran (Ace-DEX), and the coencapsulation of 3′3′-cGAMP and R848 trended toward enhanced ovalbumin-specific humoral immunity (IgG and IgG1) as compared to the individually encapsulated adjuvants. In contrast to our studies, the release kinetics of 3′3′-cGAMP or R848 were similar to coencapsulated Ace-DEX.[55] Furthermore, our use of multiparameter flow cytometry on both splenocytes and dLN-derived cells demonstrated a unique age-specific response in vivo to licensed influenza vaccine. Such responses cannot be fully replicated via the use of an ovalbumin-specific response, as quantified by the ELISpot assay or by ELISA using supernatant from protein-stimulated murine splenocytes.[55]

Overall, our study features several strengths, including (1) use of primary murine and human DCs to model individual and combined adjuvant effects in vitro, (2) assessment and demonstration of age-specific synergy of the combined engagement of STING and TLR7/8 to drive robust activation of neonatal DCs, (3) mechanistic demonstration of a precision expansion of early-life Th1 cells via the IL-12/IFNγ axis, and (4) assessment of the individual and combined effects of the adjuvants in mice in vivo. Our study also has several limitations, including (1) the potential effects of cGAMP-PS and CL075-PS on GCs are intriguing, but we might have captured delayed GC B cells and T_{FH} responses,[56] (2) although our studies demonstrated robust enhancement of immunogenicity with cGAMP-PS and CL075-PS together, future functional studies (e.g., pathogen challenge) are required to assess the efficacy of this adjuvantation approach, and (3) due to species specificity, in vivo results in mice may not accurately reflect in vivo effects in humans and would be further required to supported by porcine and/or nonhuman primate studies.

The flexibility and adaptability of the PS technology can be leveraged to fine-tune vaccine immunogenicity via targeted antigen or small-molecule adjuvant delivery and may represent a multifunctional platform for precision vaccine design in the 21st century. Such an approach must account for tailoring

https://doi.org/10.1021/acschembio.2c00497
ACS Chem. Biol. 2022, 17, 2559−2571

vaccines to vulnerable populations with distinct immunity. For example, receptor-binding domain (RBD) protein and MPLA can be formulated into stable, biologically active PSs and can induce robust RBD-specific humoral and polyfunctional Th1 responses in adult mice.[57] However, adjuvantation systems such as AS01 and AS02, both consisting of MPLA and the purified plant bark extract/saponin QS21, are components of the Mosquirix (RTS,S) malaria vaccine,[58] which has demonstrated a reduced efficacy in the pediatric setting.[58,59]

In conclusion, we demonstrate that individually encapsulated and admixed cGAMP-PS and CL075-PS shape the quantity and quality of neonatal immune responses and Th1 polarized neonatal rHA-specific humoral and cell-mediated immune responses, presenting a promising adjuvant approach for early-life immunization. Since we employed the recombinant hemagglutinin influenza vaccine throughout our work, our results may be applicable to early-life influenza immunization. The use of age-specific in vitro and in vivo modeling may also represent a general strategy for optimizing type 1 immunity toward protein antigens for early-life immunization against intracellular pathogens including additional respiratory viruses such as coronaviruses.

METHODS

Animals and Ethical Declaration. All experiments were conducted in accordance with relevant institutional and national guidelines, regulations, and approvals. All experiments involving animals were approved by the Institutional Animal Care and Use Committees (IACUC) of Boston Children's Hospital and Harvard Medical School (protocol numbers 19-02-3792R and 19-02-3897R). C57BL/6 mice (either 6−8 weeks or pregnant) were obtained from Jackson Laboratories (Bar Harbor, ME) and housed in specific pathogen-free conditions in the animal research facilities at Boston Children's Hospital. Cages were checked daily to assess the presence of pups. Discovery of a new litter was recorded as DOL 0. Both male and female pups were used for neonatal experiments in a littermate-controlled specific manner. CO_2 was used as the primary euthanasia method, with cervical dislocation as a secondary physical method to ensure death.

Nonidentifiable human cord blood samples were collected with the approval from the Ethics Committee of The Brigham & Women's Hospital, Boston, MA; Institutional Review Board (IRB) protocol number 2000-P-000117, and Beth Israel Deaconess Medical Center Boston, MA (IRB protocol number 2011P-000118). Blood samples from adult volunteers were collected after written informed consent with the approval from the Ethics Committee of Boston Children's Hospital, Boston, MA (IRB protocol number X07-05-0223).

Murine Bone Marrow-Derived Dendritic Cell (BMDC) Assay. BMDCs were generated from newborn (7 days old) and adult (6−12 weeks old) C57BL/6 mice with an adaptation of previously described methods.[13,60,61] Briefly, mice were sacrificed followed by the surgical removal of femurs and tibiae. Bones were surgically cleaned from the surrounding tissue, extremities of tibiae and femurs were trimmed with sterile scissors, and bone marrow was flushed through a 70 μm nylon mesh strainer (Corning Life Sciences). Cell number and viability were determined by the trypan blue exclusion method. Whole bone marrow cells were plated into nontissue culture-treated 100 mm Petri dishes (Corning Life Sciences) at a density of 0.3×10^6 cells/mL in 10 mL of total volume/plate of complete culture medium RPMI 1640 plus 10% heat-inactivated fetal bovine serum (FBS, GE Healthcare HyClone), 50 μM of 2-mercaptoethanol, 2 mM of L-glutamine, and 100 U/mL of penicillin/streptomycin (Gibco Thermo Fisher Scientific) supplemented with 20 ng/mL of recombinant murine GM-CSF (rmGM-CSF, R&D systems). Plates were incubated in a humidified atmosphere at 37 °C, 5% CO_2 for 6 days, with one supplement of 10 mL of complete culture medium and rmGM-CSF on day 3. On day 6, nonadherent and loosely adherent cells were harvested by washing the plate gently with a culture medium. Adherent cells were discarded.

For stimulation experiments, immature BMDCs generated from 7 days old and adult mice were plated in round-bottom 96-well nontissue culture-treated plates at a density of 10^5 cells/well in 200 μL of fresh complete culture medium with rmGM-CSF, as described above, with the appropriate stimuli. Cells were incubated at 37 °C for 20−24 h, then the supernatant was harvested, and TNF and IL-12p70 concentrations were measured by ELISA (R&D Systems). IFNβ was measured with a bioluminescent ELISA kit (LumiKine, Invivogen). For experiments involving blocking antibodies (Abs), BMDCs were preincubated for 20 min at 37 °C with antimouse IFNAR1 (clone MAR1−5A3, 10 μg/mL, Biolegend), antimouse IL-12p40, or antimouse IL-12p70 Abs or an isotype control before stimulation.

Human Monocyte-Derived Dendritic Cell (MoDC) Assay. Following local IRB-approved protocols, peripheral blood was collected from healthy adult volunteers, while human newborn cord blood was collected immediately after the cesarean section delivery of the placenta. Births to known HIV-positive mothers were excluded. Human blood was anticoagulated with 20 units/mL of pyrogen-free sodium heparin (American Pharmaceutical Partners, Inc.; Schaumberg, IL). All blood products were kept at room temperature (RT) and processed within 4 h of collection. Primary human PBMCs and CBMCs were isolated from fresh blood via Ficoll gradient separation.

Monocytes were isolated from PBMC and CBMC fractions via positive selection by magnetic microbeads according to the manufacturer's instructions (Miltenyi Biotec, Auburn, CA) using CD14 as a pan marker. Isolated monocytes were cultured in tissue culture dishes at 0.4×10^6 cells/mL in RPMI 1640 media containing fresh 10% autologous plasma, supplemented with recombinant human IL-4 (50 ng/mL) and recombinant human GM-CSF (100 ng/mL) (R&D Systems, Minneapolis, MN) with one additional supplement of fresh media and cytokines at day 3 of culture, as previously described.[12,49] After 6 days, immature MoDCs were harvested by gently pipetting the loosely adherent fraction, before being replated (10^5 cells/well) in 96-well flat-bottom plates in the presence or absence of TLRs and/or sterile PBS. Plates were then incubated for 18−24 h at 37 °C in a humidified incubator at 5% CO_2. After this stimulation, supernatants were harvested and processed for further functional assays.

Human Newborn Cord Blood Mononuclear Cell (CBMC) Stimulation. Human newborn cord blood mononuclear cells (CBMCs), containing a T cell compartment largely composed of naïve T cells, were plated at 10^5 cells/well in 96-well tissue culture plates and stimulated with aqueous formulations of indicated compounds in the presence of the polyclonal T cell activator αCD3 (plate-bound, 5 μg/mL) for 96 h. Culture supernatants were harvested and analyzed for IFNγ induction using via IFNγ ELISA (InvivoGen). For some experiments, CBMCs were stimulated with agonists alone or in combination with a mitogen (PMA/Ionomycin) and cytokine blocker for the last 6 h. After stimulation, cells were harvested and stained with surface markers followed by intracellular cytokine markers, as described in Table S2 as previously described.[13] Stained cells were analyzed by flow cytometer to quantify the percentage of T cells producing IL-4, IL-17, and IFNγ.

Nanocarrier Formulations. A range of PS formulations were prepared using the PEG-*b*-PPS block copolymer, including blank (unloaded)-PS and PS loaded with CL075, cGAMP, and CL075 + cGAMP (Table S1). PS nanocarriers were prepared by the flash nanoprecipitation technique utilizing a confined-impingement (CIJ) mixer, as published earlier.[7] Here, the organic phase was prepared by dissolving 20 mg of PEG-*b*-PPS polymer in 500 μL of tetrahydrofuran (THF) and 200 μg of CL075, while the aqueous phase was prepared by dissolving 2 mg of cGAMP in phosphate-buffered saline (PBS, pH 7.4). Organic and aqueous phases were separately loaded into syringes and impinged against each other into 2 mL of aqueous reservoir containing PBS. THF was removed from the formulation using overnight vacuum desiccation. PS was then purified to remove the unencapsulated CL075 and cGAMP using Sephadex LH-20 and Sepharose CL-6B columns, respectively. For blank-PS, organic and

https://doi.org/10.1021/acschembio.2c00497
ACS Chem. Biol. 2022, 17, 2559−2571

aqueous phases were added without adjuvants, whereas a single adjuvant-loaded PS contained the adjuvant of interest either in organic or in the aqueous phase.

Size and Morphological Characterization of Polymersomes. Dynamic light scattering (DLS) analysis was performed using a Zetasizer Nano-ZS (Malvern Instruments, U.K.) to measure the size of PS. All samples were diluted 1 in 1000 with PBS prior to the analysis.

For cryogenic transmission electron microscopy (Cryo-TEM) studies, a Pelco easiGlow glow discharger (Ted Pella) was used to glow discharge the lacey carbon Cu grids (200 mesh) at a 15 mA atmosphere plasma. The grids were applied with a 4 μL volume of the PS sample, blotted for 5 s, and plunged into liquid ethane within an FEI Vitrobot Mark III plunge freezing instrument (Thermo Fisher Scientific). Grids were stored in liquid nitrogen. Grids were viewed on a JOEL JEM1230 LaB6 emission TEM (JOEL) at 100 keV, and micrographs were obtained using a Gatan Orius SC1000 CCD camera Model 831 (Gatan).

Small-angle X-ray scattering (SAXS) studies were performed at the DuPont-Northwestern-Dow Collaborative Access Team (DND-CAT) beamline at Argonne National Laboratory's Advanced Photon Source (Argonne, IL). Collimated X-rays with 10 keV (wavelength λ = 1.24 Å) were utilized to measure the samples. Sample measurement was performed in a q-range of 0.001−0.5 $Å^{-1}$, which was calibrated using silver behenate. The final scattering data of samples were obtained using PRIMUS 2.8.2 software after subtracting the solvent buffer scattering from sample scattering. The morphologic characteristics of PS samples were confirmed after fitting the vesicle model with sample scattering data in SasView 4.0 software.

Encapsulation of CL075 and cGAMP in PS was measured after purifying PS with size exclusion chromatography and efficiency reported as mean ± SD (n = 3). The purified adjuvant-loaded PS samples obtained as mentioned above were lyophilized to rupture the nanocarrier structure. For CL075 samples, the lyophilized samples were dissolved in HPLC-grade DMF and encapsulation was measured by means of HPLC−UV/fluorescence against known standards with a dimethylformamide mobile phase, as previously described.[12] Each formulation batch was stored at −20 °C until the day of use. For cGAMP, lyophilized samples were added with methanol to precipitate the PEG-*b*-PPS block copolymer and dissolve cGAMP. The polymer precipitate was removed via centrifugation, and supernatants containing cGAMP were quantified using the liquid chromatography−mass spectrometry (LC-MS) method, as previously described.[62]

Immunization and rHA-Specific Antibody Quantification. For neonatal mouse studies, 6 days old pups were toe-clipped for individual recognition, and 7 days old C57BL/6 mice were immunized with a prime-boost schedule (two injections, each 1 week apart, for newborn mice at DOL 7 and 14). Neonatal mice were immunized i.m. in the posterior thigh with 50 μL of total vaccine dose, separated across both hind legs (25 μL per leg) according to Table S1. Each 50 μL of vaccine dose was included 1 μg of each of the following recombinant influenza virus hemagglutinins (rHA): A/Hawaii/70/2019 (H1N1), A/Minnesota/41/2019 (an A/Hong Kong/45/2019-like virus) (H3N2), B/Washington/02/2019, and B/Phuket/3073/2013 contained in the 2020−2021 formulation of the Flublok vaccine (Protein Sciences Corp). Serum was harvested 7 days following boost (DOL 21) via retroorbital bleed. Anti-rHA serum total IgG titers, IgG1 and IgG2c were measured by ELISA. During the immunization or retroorbital bleed, mice were anesthetized with isoflurane.

For anti-rHA ELISAs, CoStar 96-well high-binding plates (Corning, Corning, NY) were coated with 1 μg/mL of rHA in carbonate buffer pH 9.6, incubated overnight at 4 °C, washed 3× with wash buffer (KPL 10× phosphate-buffered saline with 0.05% Tween 20 (Fisher Scientific)), and blocked with Superblock (ScyTek) for 1 h at RT. Then, sera from vaccinated mice were added with an initial dilution of 1:100 and 1:2 serial dilutions in EIA buffer (PBS + BSA 1% + Tween 20 0.1% + heat-inactivated FBS 10%) and incubated for 2 h at RT. Plates were then washed 3× and incubated for 1 h at RT with HRP-conjugated antimouse IgG, IgG1, or IgG2c (Southern Biotech). At the end of the incubation, plates were washed 5× and developed with the BD OptEIA TMB substrate reagent set (BD, San Jose, CA) for 10 min and then stopped with 1 M H_2SO_4. The optical density was measured at 450 nm with a SpectraMax ID3 microplate reader with SoftMax Pro Version 5 (both from molecular devices), and either titers or concentrations were calculated using as cutoff three times the optical density of the background.

Cell-Mediated Immune Responses Ex Vivo. Twelve days post booster immunization (DOL 26), murine spleens were collected in RPMI 1640 media containing 10% heat-inactivated FBS. For the analysis of single-cell suspensions, spleens were mechanically and aseptically dissociated with the back of a syringe plunger and filtered through a 70 μm cell strainer and the dissociated tissue was collected in RPMI 1640 media. After centrifugation (500g, 10 min, RT), cells were treated with a 1 mL ACK lysis buffer (Gibco, Waltham, MA) for 2 min at RT to lyse red blood cells. Cells were washed immediately with RPMI 1640, passed through a 70 μm cell strainer, and suspended in RPMI 1640 media (supplemented with 10% heat-inactivated FBS). Splenocytes were plated at a density of up to 2 × 10^6 cells/well in a 96-well U-bottom plate and stimulated with 10 μg/mL of rHA (Flublok, 2020−21 formulation) in T cell media. T cell media consists of RPMI 1640 (Gibco, Waltham, MA) supplemented with 10% heat-inactivated FBS (Cytiva HyClone, Fischer Scientific), 100 U/mL of penicillin, 100 mg/mL of streptomycin (Gibco, Waltham, MA), 55 mM of 2-mercaptoethanol (Gibco, Waltham, MA), 60 mM of nonessential amino acids (Gibco, Waltham, MA), 11 mM of HEPES (Gibco, Waltham, MA), and 800 mM of L-glutamine (Gibco, Waltham, MA). In addition to antigen, the stimulation cocktail consisted of 1 μg/mL antimouse CD28/49d (BD Biosciences) as a costimulant.

For intracellular cytokine staining (ICS), 18 h of stimulation was completed in a humidified incubator at 37 °C, 5% CO_2 and 5 μg/mL of Brefeldin A (BFA; BioLegend) was added during the last 6 h of stimulation to block the cytokine production and facilitate the optimal intracellular flow cytometry analysis. After 18 h of stimulation, cells were washed twice with PBS and blocked with a mouse Fc block (BD Biosciences) according to the manufacturer's instructions. After blocking, cells were washed once with PBS and stained with aqua live/dead stain (Life Technologies, Carlsbad, CA) for 15 min at RT. Following two additional PBS washes, cells were resuspended in 100 μL of FACS buffer (PBS supplemented with 0.2% BSA (Sigma-Aldrich)) containing mouse-specific cell surface markers for flow cytometry. Markers included antimouse CD44 PerCP-Cy5.5, CD3 BV785, CD4 APC/Fire750, and CD8 BUV395. Details of the clone and manufacturer of each marker used in a customized eight-color flow cytometry panel are documented in Table S2. Cells were incubated with the surface markers for 30 min at 4 °C. Cells were washed with PBS and fixed/permeabilized using the BD Cytofix/Cytoperm fixation/permeabilization solution kit according to the manufacturer's instructions. Cells were washed in 1× perm/wash solution and subjected to intracellular staining (30 min at 4 °C) using a cocktail of the following Abs: antimouse IFNγ Alexa Fluor 488, TNF PE Cy7, and IL-2 PE in 1× perm/wash solution. Finally, cells were washed in PBS and fixed in PBS containing 1% paraformaldehyde (Electron Microscopy Sciences, Hatfield, PA) for 20 min at 4 °C. After two final washes in PBS, the cells were resuspended in PBS and stored at 4 °C until acquisition. Samples were acquired on a BD LSRFortessa (BD Biosciences; San Jose, CA) configured with blue (488 nm), yellow/green (568 nm), red (640 nm), violet (407 nm), and ultraviolet (355 nm) lasers using standardized good clinical laboratory practice procedures to minimize the variability of data generated. Analysis was performed using FlowJo software, v.10.8.1, according to the gating strategy outlined in Figures S2A and S3A.

T_{FH} and B Cell Responses in Draining Lymph Nodes. Draining (inguinal and popliteal) lymph nodes (dLNs) from mice were harvested 12 days post boost (DOL 26), as previously reported.[13] To prepare a single-cell suspension, dLNs were mechanically and aseptically dissociated with the back of a syringe plunger and filtered through a 70 μm cell strainer and collected in

https://doi.org/10.1021/acschembio.2c00497
ACS Chem. Biol. 2022, 17, 2559−2571

RPMI 1640 media. Then, cells were washed and stained with the Abs (described in Table S2), as previously reported.[63] The gating strategy is shown in Figure S4A. T_{FH} cells in DLNs were phenotyped as $CD3^+CD4^+PD\text{-}1^+CXCR5^+$, GC B cells as $CD3^-CD19^+CD95^+GL7^+$, plasmablasts as $CD3^-CD19^+$ $CD138^+$, and plasma cells as $CD3^-CD19^-CD138^+$ by using a customized flow cytometry panel. Details of the clone, manufacturer, and titer of each marker are documented in Table S2.

Statistical Analyses and Graphics. Statistical significance and graphic output were generated using the GraphPad Prism version 9.3.1 for macOS (GraphPad Software, La Jolla, CA). Data were tested for normality using the Shapiro−Wilk test. Group comparisons were performed by one or two-way ANOVA with Dunnett's or Tukey's multiple comparison post-test. Measurements that failed normality tests were analyzed with a Kruskal−Wallis rank-sum test followed by Dunn's multiple comparison within treatment groups. Results were considered significant at p values indicated in each figure legend. Synergy was calculated using an adaptation of the Loewe method of additivity, as previously described.[30] D values greater than one were considered antagonistic, D values equal to one were considered additive, and D values less than one were considered synergistic. Analysis and presentation of flow cytometric data (Figure S3B) were performed using SPICE (Ver. 6; https://niaid.github.io/spice/).[64,65] Graphics in abstract, Figures 3A, 4A, 5B, and S4B were created with BioRender.com.

■ ASSOCIATED CONTENT

Supporting Information

The Supporting Information is available free of charge at https://pubs.acs.org/doi/10.1021/acschembio.2c00497.

rHA-specific humoral and cell-mediated responses (Figures S1−S3 and S5); T_{FH} and B cell responses in DLN (Figure S4); vaccine formulations for in vivo study (Table S1); and flow cytometry reagents (Table S2) (PDF)

■ AUTHOR INFORMATION

Corresponding Authors

Evan A. Scott − *Department of Biomedical Engineering, Northwestern University, Chicago, Illinois 60208, United States;* orcid.org/0000-0002-8945-2892; Email: evan.scott@northwestern.edu

David J. Dowling − *Precision Vaccines Program, Division of Infectious Diseases, Boston Children's Hospital, Boston, Massachusetts 02115, United States; Harvard Medical School, Boston, Massachusetts 02115, United States;* orcid.org/0000-0003-1095-6156; Phone: 617-919-2906; Email: david.dowling@childrens.harvard.edu

Authors

Soumik Barman − *Precision Vaccines Program, Division of Infectious Diseases, Boston Children's Hospital, Boston, Massachusetts 02115, United States; Harvard Medical School, Boston, Massachusetts 02115, United States;* orcid.org/0000-0002-3641-2125

Francesco Borriello − *Precision Vaccines Program, Division of Infectious Diseases, Boston Children's Hospital, Boston, Massachusetts 02115, United States; Harvard Medical School, Boston, Massachusetts 02115, United States; Department of Translational Medical Sciences and Center for Basic and Clinical Immunology Research (CISI), University of Naples Federico II, Naples 80131, Italy; WAO Center of Excellence, Naples 80131, Italy;* Present Address: Generate Biomedicines, Cambridge, Massachusetts 02142, United States

Byron Brook − *Precision Vaccines Program, Division of Infectious Diseases, Boston Children's Hospital, Boston, Massachusetts 02115, United States; Harvard Medical School, Boston, Massachusetts 02115, United States;* orcid.org/0000-0003-3184-8285

Carlo Pietrasanta − *Precision Vaccines Program, Division of Infectious Diseases, Boston Children's Hospital, Boston, Massachusetts 02115, United States; Harvard Medical School, Boston, Massachusetts 02115, United States; Fondazione IRCCS Ca' Granda Ospedale Maggiore Policlinico, NICU, Milan 20122, Italy; Department of Clinical Sciences and Community Health, University of Milan, Milan 20122, Italy*

Maria De Leon − *Precision Vaccines Program, Division of Infectious Diseases, Boston Children's Hospital, Boston, Massachusetts 02115, United States;* orcid.org/0000-0001-6730-3442

Cali Sweitzer − *Precision Vaccines Program, Division of Infectious Diseases, Boston Children's Hospital, Boston, Massachusetts 02115, United States*

Manisha Menon − *Precision Vaccines Program, Division of Infectious Diseases, Boston Children's Hospital, Boston, Massachusetts 02115, United States*

Simon D. van Haren − *Precision Vaccines Program, Division of Infectious Diseases, Boston Children's Hospital, Boston, Massachusetts 02115, United States; Harvard Medical School, Boston, Massachusetts 02115, United States*

Dheeraj Soni − *Precision Vaccines Program, Division of Infectious Diseases, Boston Children's Hospital, Boston, Massachusetts 02115, United States; Harvard Medical School, Boston, Massachusetts 02115, United States*

Yoshine Saito − *Precision Vaccines Program, Division of Infectious Diseases, Boston Children's Hospital, Boston, Massachusetts 02115, United States*

Etsuro Nanishi − *Precision Vaccines Program, Division of Infectious Diseases, Boston Children's Hospital, Boston, Massachusetts 02115, United States; Harvard Medical School, Boston, Massachusetts 02115, United States*

Sijia Yi − *Department of Biomedical Engineering, Northwestern University, Chicago, Illinois 60208, United States;* Present Address: Merck, Pennsylvania, Lansdale, Pennsylvania 19446, United States

Sharan Bobbala − *Department of Pharmaceutical Sciences, School of Pharmacy, West Virginia University, Morgantown, West Virginia 26506, United States*

Ofer Levy − *Precision Vaccines Program, Division of Infectious Diseases, Boston Children's Hospital, Boston, Massachusetts 02115, United States; Harvard Medical School, Boston, Massachusetts 02115, United States; Broad Institute of MIT & Harvard, Cambridge, Massachusetts 02142, United States*

Complete contact information is available at: https://pubs.acs.org/10.1021/acschembio.2c00497

Author Contributions

⋈F.B., B.B., C.P. (for co-second authorship), * E.A.S., and D.J.D. (for correspondance) contributed equally to this work. S.B. (Barman) and D.J.D. designed the experiments, prepared the figures, and wrote the manuscript. F.B. and C.P. performed in vitro experiments, flow cytometry (human samples), and assisted with data analysis. S.B. (Bobbala), S.Y., and E.A.S. synthesized and characterized adjuvant-loaded nanocarriers. B.B. precipitated in the animal experiments and organ

https://doi.org/10.1021/acschembio.2c00497
ACS Chem. Biol. 2022, 17, 2559−2571

harvesting. C.S., M.M., and D.S. helped B.B. and S.B. (Barman) during the preparation of single-cell suspension from the harvested organs. S.B. (Barman) performed the flow cytometry (mice samples) assay and analyzed the data. M.D.L., Y.S., E.N., and D.S. participated in the experiments related to vaccine-induced humoral responses. S.v.H. and O.L. edited and critically reviewed the manuscript. E.A.S., O.L., and D.J.D. conceived the project, secured funding, and supervised the study. All authors reviewed and edited the manuscript.

Funding

D.J.D.'s laboratory was supported by NIH grant 1R21AI137932-01A1. Both D.J.D. and O.L.'s laboratory were supported by Adjuvant Discovery Program (75N93019C00044), Adjuvant Development Program (272201800047C), and Development of Vaccines for the Treatment of Opioid Use Disorder (272201800047C-P00003-9999). The *Precision Vaccines Program* is supported, in part, by the Boston Children's Hospital, Department of Pediatrics. C.P. was supported by the scholarship "J. Miglierina", Fondazione Comunitaria del Varesotto, Varese, Italy.

Notes

The authors declare the following competing financial interest(s): EN, FB, BB, DS, SvH, OL and DJD are named inventors on vaccine adjuvant patents assigned to Boston Childrens Hospital. FB has signed consulting agreements with Merck Sharp & Dohme Corp. (a subsidiary of Merck & Co., Inc.), Sana Biotechnology, Inc., and F. Hoffmann-La Roche Ltd. IZ reports compensation for consulting services with Implicit Biosciences. The rest of the authors do not have any competing interests.

■ ACKNOWLEDGMENTS

The authors thank the members of the *Precision Vaccines Program* for helpful discussions as well as K. Churchwell, G. Fleisher, D. Williams, and A. Cervini for their support of the Precision Vaccines Program. D.J.D. would like to thank S. McHugh, G. Boyer, L. Conetta, and the staff of Lucy's Daycare, the staff of the YMCA of Greater Boston, Bridging Independent Living Together (BILT), Inc., and the Boston Public Schools for childcare and educational support during the COVID-19 pandemic.

■ REFERENCES

(1) Barman, S.; Soni, D.; Brook, B.; Nanishi, E.; Dowling, D. J. Precision Vaccine Development: Cues From Natural Immunity. *Front. Immunol.* **2022**, *12*, No. 662218.

(2) Ong, G. H.; Lian, B. S. X.; Kawasaki, T.; Kawai, T. Exploration of Pattern Recognition Receptor Agonists as Candidate Adjuvants. *Front. Cell Infect. Microbiol.* **2021**, *11*, No. 745016.

(3) Dowling, D. J. Recent Advances in the Discovery and Delivery of TLR7/8 Agonists as Vaccine Adjuvants. *Immunohorizons* **2018**, *2*, 185−197.

(4) Rapaka, R. R.; Cross, A. S.; McArthur, M. A. Using Adjuvants to Drive T Cell Responses for Next-Generation Infectious Disease Vaccines. *Vaccines* **2021**, *9*, No. 820.

(5) Soni, D.; Bobbala, S.; Li, S.; Scott, E. A.; Dowling, D. J. The sixth revolution in pediatric vaccinology: immunoengineering and delivery systems. *Pediatr. Res.* **2021**, *89*, 1364−1372.

(6) Bachmann, M. F.; Jennings, G. T. Vaccine delivery: a matter of size, geometry, kinetics and molecular patterns. *Nat. Rev. Immunol.* **2010**, *10*, 787−796.

(7) Allen, S.; Osorio, O.; Liu, Y. G.; Scott, E. Facile assembly and loading of theranostic polymersomes via multi-impingement flash nanoprecipitation. *J. Control Release* **2017**, *262*, 91−103.

(8) Bobbala, S.; Allen, S. D.; Scott, E. A. Flash nanoprecipitation permits versatile assembly and loading of polymeric bicontinuous cubic nanospheres. *Nanoscale* **2018**, *10*, 5078−5088.

(9) Shang, S.; Kats, D.; Cao, L.; Morgun, E.; Velluto, D.; He, Y.; Xu, Q.; Wang, C. R.; Scott, E. A. Induction of *Mycobacterium Tuberculosis* Lipid-Specific T Cell Responses by Pulmonary Delivery of Mycolic Acid-Loaded Polymeric Micellar Nanocarriers. *Front. Immunol.* **2018**, *9*, 2709.

(10) Vincent, M. P.; Bobbala, S.; Karabin, N. B.; Frey, M.; Liu, Y.; Navidzadeh, J. O.; Stack, T.; Scott, E. A. Surface chemistry-mediated modulation of adsorbed albumin folding state specifies nanocarrier clearance by distinct macrophage subsets. *Nat. Commun.* **2021**, *12*, No. 648.

(11) Burke, J. A.; Zhang, X.; Bobbala, S.; Frey, M. A.; Bohorquez Fuentes, C.; Freire Haddad, H.; Allen, S. D.; Richardson, R. A. K.; Ameer, G. A.; Scott, E. A. Subcutaneous nanotherapy repurposes the immunosuppressive mechanism of rapamycin to enhance allogeneic islet graft viability. *Nat. Nanotechnol.* **2022**, *17*, 319−330.

(12) Dowling, D. J.; Scott, E. A.; Scheid, A.; Bergelson, I.; Joshi, S.; Pietrasanta, C.; Brightman, S.; Sanchez-Schmitz, G.; Van Haren, S. D.; Ninkovic, J.; et al. Toll-like receptor 8 agonist nanoparticles mimic immunomodulating effects of the live BCG vaccine and enhance neonatal innate and adaptive immune responses. *J. Allergy Clin. Immunol.* **2017**, *140*, 1339−1350.

(13) Borriello, F.; Pietrasanta, C.; Lai, J. C. Y.; Walsh, L. M.; Sharma, P.; O'Driscoll, D. N.; Ramirez, J.; Brightman, S.; Pugni, L.; Mosca, F.; et al. Identification and Characterization of Stimulator of Interferon Genes As a Robust Adjuvant Target for Early Life Immunization. *Front. Immunol.* **2017**, *8*, 1772.

(14) Benoit-Lizon, I.; Jacquin, E.; Vargas, T. R.; Richard, C.; Roussey, A.; Dal Zuffo, L.; Martin, T.; Melis, A.; Vinokurova, D.; Shahoei, S. H.; et al. CD4 T cell-intrinsic STING signaling controls the differentiation and effector functions of TH1 and TH9 cells. *J. Immunother. Cancer* **2022**, *10*, No. e003459.

(15) Van Herck, S.; Feng, B.; Tang, L. Delivery of STING agonists for adjuvanting subunit vaccines. *Adv. Drug Delivery Rev.* **2021**, *179*, No. 114020.

(16) Napolitani, G.; Rinaldi, A.; Bertoni, F.; Sallusto, F.; Lanzavecchia, A. Selected Toll-like receptor agonist combinations synergistically trigger a T helper type 1-polarizing program in dendritic cells. *Nat. Immunol.* **2005**, *6*, 769−776.

(17) Roßmann, L.; Bagola, K.; Stephen, T.; Gerards, A. L.; Walber, B.; Ullrich, A.; Schulke, S.; Kamp, C.; Spreitzer, I.; Hasan, M.; David-Watine, B. Distinct single-component adjuvants steer human DC-mediated T-cell polarization via Toll-like receptor signaling toward a potent antiviral immune response. *Proc. Natl. Acad. Sci. U.S.A.* **2021**, *118*, No. e2103651118.

(18) Darling, R. J.; Senapati, S.; Kelly, S. M.; Kohut, M. L.; Narasimhan, B.; Wannemuehler, M. J. STING pathway stimulation results in a differentially activated innate immune phenotype associated with low nitric oxide and enhanced antibody titers in young and aged mice. *Vaccine* **2019**, *37*, 2721−2730.

(19) Lioux, T.; Mauny, M. A.; Lamoureux, A.; Bascoul, N.; Hays, M.; Vernejoul, F.; Baudru, A. S.; Boularan, C.; Lopes-Vicente, J.; Qushair, G.; Tiraby, G. Design, Synthesis, and Biological Evaluation of Novel Cyclic Adenosine-Inosine Monophosphate (cAIMP) Analogs That Activate Stimulator of Interferon Genes (STING). *J. Med. Chem.* **2016**, *59*, 10253−10267.

(20) Dowling, D. J.; Tan, Z.; Prokopowicz, Z. M.; Palmer, C. D.; Matthews, M. A.; Dietsch, G. N.; Hershberg, R. M.; Levy, O. The ultra-potent and selective TLR8 agonist VTX-294 activates human newborn and adult leukocytes. *PLoS One* **2013**, *8*, No. e58164.

(21) Wenner, C. A.; Guler, M. L.; Macatonia, S. E.; O'Garra, A.; Murphy, K. M. Roles of IFN-gamma and IFN-alpha in IL-12-induced T helper cell-1 development. *J. Immunol.* **1996**, *156*, 1442−1447.

(22) Short, K. K.; Miller, S. M.; Walsh, L.; Cybulski, V.; Bazin, H.; Evans, J. T.; Burkhart, D. Co-encapsulation of synthetic lipidated TLR4 and TLR7/8 agonists in the liposomal bilayer results in a rapid,

https://doi.org/10.1021/acschembio.2c00497
ACS Chem. Biol. 2022, 17, 2559−2571

synergistic enhancement of vaccine-mediated humoral immunity. *J. Control Release* **2019**, *315*, 186−196.
(23) Lemoine, S.; Jaron, B.; Tabka, S.; Ettreiki, C.; Deriaud, E.; Zhivaki, D.; Le Ray, C.; Launay, O.; Majlessi, L.; Tissieres, P.; et al. Dectin-1 activation unlocks IL12A expression and reveals the TH1 potency of neonatal dendritic cells. *J. Allergy Clin. Immunol.* **2015**, *136*, 1355−1368.
(24) Surendran, N.; Simmons, A.; Pichichero, M. E. TLR agonist combinations that stimulate Th type I polarizing responses from human neonates. *Innate Immun.* **2018**, *24*, 240−251.
(25) Adkins, B.; Bu, Y.; Guevara, P. The generation of Th memory in neonates versus adults: prolonged primary Th2 effector function and impaired development of Th1 memory effector function in murine neonates. *J. Immunol.* **2001**, *166*, 918−925.
(26) Argondizo-Correia, C.; Rodrigues, A. K. S.; de Brito, C. A. Neonatal Immunity to Bordetella pertussis Infection and Current Prevention Strategies. *J. Immunol. Res.* **2019**, *2019*, No. 7134168.
(27) Tang, J.; Wennerberg, K.; Aittokallio, T. What is synergy? The Saariselka agreement revisited. *Front. Pharmacol.* **2015**, *6*, No. 181.
(28) Loewe, S. The problem of synergism and antagonism of combined drugs. *Arzneimittelforschung* **1953**, *3*, 285−290.
(29) Fitzgerald, J. B.; Schoeberl, B.; Nielsen, U. B.; Sorger, P. K. Systems biology and combination therapy in the quest for clinical efficacy. *Nat. Chem. Biol.* **2006**, *2*, 458−466.
(30) van Haren, S. D.; Dowling, D. J.; Foppen, W.; Christensen, D.; Andersen, P.; Reed, S. G.; Hershberg, R. M.; Baden, L. R.; Levy, O. Age-Specific Adjuvant Synergy: Dual TLR7/8 and Mincle Activation of Human Newborn Dendritic Cells Enables Th1 Polarization. *J. Immunol.* **2016**, *197*, 4413−4424. From NLM Medline.
(31) Scott, E. A.; Stano, A.; Gillard, M.; Maio-Liu, A. C.; Swartz, M. A.; Hubbell, J. A. Dendritic cell activation and T cell priming with adjuvant- and antigen-loaded oxidation-sensitive polymersomes. *Biomaterials* **2012**, *33*, 6211−6219.
(32) Cerritelli, S.; O'Neil, C. P.; Velluto, D.; Fontana, A.; Adrian, M.; Dubochet, J.; Hubbell, J. A. Aggregation behavior of poly(ethylene glycol-bl-propylene sulfide) di- and triblock copolymers in aqueous solution. *Langmuir* **2009**, *25*, 11328−11335.
(33) Khurana, S.; Hahn, M.; Coyle, E. M.; King, L. R.; Lin, T. L.; Treanor, J.; Sant, A.; Golding, H. Repeat vaccination reduces antibody affinity maturation across different influenza vaccine platforms in humans. *Nat. Commun.* **2019**, *10*, No. 3338.
(34) Richards, K. A.; Moritzky, S.; Shannon, I.; Fitzgerald, T.; Yang, H.; Branche, A.; Topham, D. J.; Treanor, J. J.; Nayak, J.; Sant, A. J. Recombinant HA-based vaccine outperforms split and subunit vaccines in elicitation of influenza-specific CD4 T cells and CD4 T cell-dependent antibody responses in humans. *npj Vaccines* **2020**, *5*, 77.
(35) Pérez-Rubio, G.; Ponce-Gallegos, M. A.; Dominguez-Mazzocco, B. A.; Ponce-Gallegos, J.; Garcia-Ramirez, R. A.; Falfan-Valencia, R. Role of the Host Genetic Susceptibility to 2009 Pandemic Influenza A H1N1. *Viruses* **2021**, *13*, No. 344.
(36) Zhang, H.; Zheng, H.; Guo, P.; Hu, L.; Wang, Z.; Wang, J.; Ju, Y.; Meng, S. Broadly Protective CD8(+) T Cell Immunity to Highly Conserved Epitopes Elicited by Heat Shock Protein gp96-Adjuvanted Influenza Monovalent Split Vaccine. *J. Virol.* **2021**, *95*, No. e00507-21.
(37) Wang, J.; Li, P.; Yu, Y.; Fu, Y.; Jiang, H.; Lu, M.; Sun, Z.; Jiang, S.; Lu, L.; Wu, M. X. Pulmonary surfactant-biomimetic nanoparticles potentiate heterosubtypic influenza immunity. *Science* **2020**, *367*, No. eaau0810.
(38) Gutjahr, A.; Papagno, L.; Nicoli, F.; Kanuma, T.; Kuse, N.; Cabral-Piccin, M. P.; Rochereau, N.; Gostick, E.; Lioux, T.; Perouzel, E.; et al. The STING ligand cGAMP potentiates the efficacy of vaccine-induced CD8+ T cells. *JCI Insight* **2019**, *4*, No. e125107.
(39) Ugolini, M.; Gerhard, J.; Burkert, S.; Jensen, K. J.; Georg, P.; Ebner, F.; Volkers, S. M.; Thada, S.; Dietert, K.; Bauer, L.; et al. Recognition of microbial viability via TLR8 drives TFH cell differentiation and vaccine responses. *Nat. Immunol.* **2018**, *19*, 386−396.
(40) Ayithan, N.; Tang, L.; Tan, S. K.; Chen, D.; Wallin, J. J.; Fletcher, S. P.; Kottilil, S.; Poonia, B. Follicular Helper T (TFH) Cell Targeting by TLR8 Signaling For Improving HBsAg-Specific B Cell Response In Chronic Hepatitis B Patients. *Front. Immunol.* **2021**, *12*, No. 735913.
(41) Chauveau, L.; Bridgeman, A.; Tan, T. K.; Beveridge, R.; Frost, J. N.; Rijal, P.; Pedroza-Pacheco, I.; Partridge, T.; Gilbert-Jaramillo, J.; Knight, M. L.; et al. Inclusion of cGAMP within virus-like particle vaccines enhances their immunogenicity. *EMBO Rep.* **2021**, *22*, No. e52447.
(42) Zhang, X.; Zhivaki, D.; Lo-Man, R. Unique aspects of the perinatal immune system. *Nat. Rev. Immunol.* **2017**, *17*, 495−507.
(43) Dowling, D. J.; Levy, O. Ontogeny of early life immunity. *Trends Immunol.* **2014**, *35*, 299−310.
(44) Merad, M.; Sathe, P.; Helft, J.; Miller, J.; Mortha, A. The dendritic cell lineage: ontogeny and function of dendritic cells and their subsets in the steady state and the inflamed setting. *Annu. Rev. Immunol.* **2013**, *31*, 563−604.
(45) Kreutz, M.; Tacken, P. J.; Figdor, C. G. Targeting dendritic cells–why bother? *Blood* **2013**, *121*, 2836−2844.
(46) Kastenmüller, W.; Kastenmuller, K.; Kurts, C.; Seder, R. A. Dendritic cell-targeted vaccines–hope or hype? *Nat. Rev. Immunol.* **2014**, *14*, 705−711.
(47) Dowling, D. J.; Scott, E. A.; Scheid, A.; Bergelson, I.; Joshi, S.; Pietrasanta, C.; Brightman, S.; Sanchez-Schmitz, G.; Van Haren, S. D.; Ninkovic, J.; Kats, D. Toll-like receptor 8 agonist nanoparticles mimic immunomodulating effects of the live BCG vaccine and enhance neonatal innate and adaptive immune responses. *J. Allergy Clin. Immunol.* **2017**, *140*, 1339−1350.
(48) Dowling, D. J.; van Haren, S. D.; Scheid, A.; Bergelson, I.; Kim, D.; Mancuso, C. J.; Foppen, W.; Ozonoff, A.; Fresh, L.; Theriot, T. B.; et al. TLR7/8 adjuvant overcomes newborn hyporesponsiveness to pneumococcal conjugate vaccine at birth. *JCI Insight* **2017**, *2*, No. e91020.
(49) Ganapathi, L.; Van Haren, S.; Dowling, D. J.; Bergelson, I.; Shukla, N. M.; Malladi, S. S.; Balakrishna, R.; Tanji, H.; Ohto, U.; Shimizu, T.; et al. The Imidazoquinoline Toll-Like Receptor-7/8 Agonist Hybrid-2 Potently Induces Cytokine Production by Human Newborn and Adult Leukocytes. *PLoS One* **2015**, *10*, No. e0134640.
(50) Levy, O.; Zarember, K. A.; Roy, R. M.; Cywes, C.; Godowski, P. J.; Wessels, M. R. Selective impairment of TLR-mediated innate immunity in human newborns: neonatal blood plasma reduces monocyte TNF-alpha induction by bacterial lipopeptides, lipopolysaccharide, and imiquimod, but preserves the response to R-848. *J. Immunol.* **2004**, *173*, 4627−4634.
(51) Levy, O.; Suter, E. E.; Miller, R. L.; Wessels, M. R. Unique efficacy of Toll-like receptor 8 agonists in activating human neonatal antigen-presenting cells. *Blood* **2006**, *108*, 1284−1290.
(52) Philbin, V. J.; Dowling, D. J.; Gallington, L. C.; Cortes, G.; Tan, Z.; Suter, E. E.; Chi, K. W.; Shuckett, A.; Stoler-Barak, L.; Tomai, M.; et al. Imidazoquinoline Toll-like receptor 8 agonists activate human newborn monocytes and dendritic cells through adenosine-refractory and caspase-1-dependent pathways. *J. Allergy Clin. Immunol.* **2012**, *130*, 195−204 e199.
(53) Kollmann, T. R.; Crabtree, J.; Rein-Weston, A.; Blimkie, D.; Thommai, F.; Wang, X. Y.; Lavoie, P. M.; Furlong, J.; Fortuno, E. S., 3rd; Hajjar, A. M.; et al. Neonatal innate TLR-mediated responses are distinct from those of adults. *J. Immunol.* **2009**, *183*, 7150−7160.
(54) Miyauchi, K.; Sugimoto-Ishige, A.; Harada, Y.; Adachi, Y.; Usami, Y.; Kaji, T.; Inoue, K.; Hasegawa, H.; Watanabe, T.; Hijikata, A.; et al. Protective neutralizing influenza antibody response in the absence of T follicular helper cells. *Nat. Immunol.* **2016**, *17*, 1447−1458.
(55) Collier, M. A.; Junkins, R. D.; Gallovic, M. D.; Johnson, B. M.; Johnson, M. M.; Macintyre, A. N.; Sempowski, G. D.; Bachelder, E. M.; Ting, J. P.; Ainslie, K. M. Acetalated Dextran Microparticles for Codelivery of STING and TLR7/8 Agonists. *Mol. Pharm.* **2018**, *15*, 4933−4946.

https://doi.org/10.1021/acschembio.2c00497
ACS Chem. Biol. 2022, 17, 2559−2571

(56) Lee, A.; Scott, M. K.; Wimmers, F.; Arunachalam, P. S.; Luo, W.; Fox, C. B.; Tomai, M.; Khatri, P.; Pulendran, B. A molecular atlas of innate immunity to adjuvanted and live attenuated vaccines, in mice. *Nat. Commun.* **2022**, *13*, No. 549.
(57) Volpatti, L. R.; Wallace, R. P.; Cao, S.; Raczy, M. M.; Wang, R.; Gray, L. T.; Alpar, A. T.; Briquez, P. S.; Mitrousis, N.; Marchell, T. M.; et al. Polymersomes Decorated with the SARS-CoV-2 Spike Protein Receptor-Binding Domain Elicit Robust Humoral and Cellular Immunity. *ACS Cent. Sci.* **2021**, *7*, 1368−1380.
(58) Laurens, M. B. RTS,S/AS01 vaccine (Mosquirix): an overview. *Hum. Vaccines Immunother.* **2020**, *16*, 480−489.
(59) Rappuoli, R.; Aderem, A. A 2020 vision for vaccines against HIV, tuberculosis and malaria. *Nature* **2011**, *473*, 463−469.
(60) Lutz, M. B.; Kukutsch, N.; Ogilvie, A. L.; Rossner, S.; Koch, F.; Romani, N.; Schuler, G. An advanced culture method for generating large quantities of highly pure dendritic cells from mouse bone marrow. *J. Immunol. Methods* **1999**, *223*, 77−92.
(61) Dowling, D.; Hamilton, C. M.; O'Neill, S. M. A comparative analysis of cytokine responses, cell surface marker expression and MAPKs in DCs matured with LPS compared with a panel of TLR ligands. *Cytokine* **2008**, *41*, 254−262.
(62) Leventhal, D. S.; Sokolovska, A.; Li, N.; Plescia, C.; Kolodziej, S. A.; Gallant, C. W.; Christmas, R.; Gao, J. R.; James, M. J.; Abin-Fuentes, A.; et al. Immunotherapy with engineered bacteria by targeting the STING pathway for anti-tumor immunity. *Nat. Commun.* **2020**, *11*, No. 2739.
(63) Sato-Kaneko, F.; Yao, S.; Lao, F. S.; Shpigelman, J.; Messer, K.; Pu, M.; Shukla, N. M.; Cottam, H. B.; Chan, M.; Chu, P. J.; et al. A Novel Synthetic Dual Agonistic Liposomal TLR4/7 Adjuvant Promotes Broad Immune Responses in an Influenza Vaccine With Minimal Reactogenicity. *Front. Immunol.* **2020**, *11*, 1207.
(64) Roederer, M.; Nozzi, J. L.; Nason, M. C. SPICE: exploration and analysis of post-cytometric complex multivariate datasets. *Cytometry, Part A* **2011**, *79A*, 167−174.
(65) Darrah, P. A.; DiFazio, R. M.; Maiello, P.; Gideon, H. P.; Myers, A. J.; Rodgers, M. A.; Hackney, J. A.; Lindenstrom, T.; Evans, T.; Scanga, C. A.; et al. Boosting BCG with proteins or rAd5 does not enhance protection against tuberculosis in rhesus macaques. *npj Vaccines* **2019**, *4*, 21.

https://doi.org/10.1021/acschembio.2c00497
ACS Chem. Biol. 2022, 17, 2559−2571